Two-Dimensional Arrays of Strings of TiO_2 Nanoparticles via Cooperative Block Copolymer Self-Assembly

Juan Peng,[†,‡] Wolfgang Knoll,*[,†] Cheolmin Park,[§] and Dong Ha Kim*[,#]

Max-Planck-Institute for Polymer Research, Ackermannweg 10, Mainz D-55128, Germany, Department of Macromolecular Science, The Key Laboratory of Molecular Engineering of Polymers, Ministry of Education, Fudan University, Shanghai 200433, China, Department of Materials Science and Engineering, Yonsei University, 134 Shinchon-Dong, Seodaemun-Gu, Seoul 120-749, Korea, and Division of Nano Sciences and Department of Chemistry, Ewha Womans University, 11-1 Daehyun-Dong, Seodaemun-Gu, Seoul 120-750, Korea

Received September 12, 2007
Revised Manuscript Received December 28, 2007

Tuning the shape and size of low-dimensional nanostructured materials in relation to their unique properties has been a critical issue in recent nanoscience and nanotechnology.[1] Nanoscale semiconductors have been widely discussed because of their novel optical, electronic, magnetic, and chemical properties. In particular, titanium dioxide (TiO_2) has been applied in a wide range of applications including as chemical sensor, as catalyst, and in solar cells.[2,3] Various routes to nanostructured TiO_2 have been reported, such as sol–gel process, pulsed laser deposition, electrodeposition, self-assembly process, and so forth.[4,5] In particular, block copolymer (BCP) templating offers a facile route to fabricate ordered TiO_2 nanostructures. [6,7] However, in most cases this methodology allows for the fabrication of regular, periodic nanostructures with characteristic lattice spacing, and the inorganic nanostructures derived from the parent BCP templates are the replica of them. Recently, Kang et al. reported a sphere-to-string transition induced by adding a surfactant into or by increasing ionic strength of an amphilic BCP micelle solution.[8] Another work has demonstrated that the organization of BCPs is forced down specific pathways into complex one-dimensional structures via kinetic control, that is, through a combination of solvent mixing and the complexation of a charged, hydrophilic block with divalent, organic counterions.[9] However, these methodologies are attended with the design of a complex BCP architecture or require multiple steps with additional ingredients in the solution. Herein, we suggest a simpler, facile process to generate two-dimensional (2D) strings of TiO_2 nanoparticles with donut-like structures based on BCP self-assembly coupled with a sol–gel process. We found that controlling the mixing protocol of the common solution is the critical step to obtain such 2D arrays of strings of inorganic nanoparticles with exquisite morphology.

In a typical experiment, poly(styrene-*block*-2-vinyl pyridine copolymer (PS-b-P2VP, $M_{n,PS} = 54\,900$ g/mol, $M_{n,P2VP} = 18\,600$ g/mol, Polymer Source, Inc.) was dissolved in benzene with a concentration of 0.5 wt %. Sol–gel precursor solution was prepared by adding concentrated HCl (37%, 0.12 g) into isopropanol (2.5 mL) containing titanium tetraisopropoxide (TTIP, 0.37 g). The molar ratio of TTIP/HCl in the sol–gel solution was 1.01. Afterward, toluene (2.3 mL) was added into the solution to dilute the sol–gel precursor and stirred for 1 h. The desired amount of sol–gel precursor solution was mixed with the PS-b-P2VP solution and stirred for 30 min. The amount of precursor solution relative to the BCP solution was adjusted from 11.6 to 58.0% (w/w). Thin films were prepared by spin-coating mixed solution onto silicon wafers at 2000 rpm for 60 s. The samples were irradiated by UV light at 254 nm for 48 h to remove the organic matrix.

It has been reported that as-cast PS-b-P2VP thin films exhibit monolayer micellar morphology with a core of P2VP block and corona of PS block in benzene which dissolves PS better than P2VP.[10] The micellar nanostructures are employed as templates to generate titania nanostructures. A series of PS-b-P2VP/titania hybrid films are obtained by spin coating mixed solution with different amounts of sol–gel precursor relative to PS-b-P2VP onto silicon wafers, as shown in Figure 1.

For the films with 11.6% sol–gel precursor, circular nanohole morphology is observed with the diameter and depth of ~30.1 and 4.1 nm, respectively, as shown in Figure 1a. When the amount of precursor is increased to 23.2%, the nanoholes became bigger where part of them became irregular (Figure 1b). If the amount of precursor is further increased to 46.4%, a novel morphology of strings of micelles with nanoholes was produced (Figure 1c). Such network structure became more ordered in the case of 58.0% precursor content (Figure 1d).

The corresponding series of FESEM images of pure titania nanostructures with different morphologies are shown in

---

[*] Corresponding author. E-mail: knoll@mpip-mainz.mpg.de (W.K.), dhkim@ewha.ac.kr (D.H.K.).
[†] Max-Planck-Institute for Polymer Research.
[‡] Fudan Unversity.
[§] Yonsei Unversity.
[#] Ewha Womans University.

(1) Xia, Y.; Yang, P.; Sun, Y.; Wu, Y.; Mayers, B.; Gates, B.; Yin, Y.; Kim, F.; Yan, H. *Adv. Mater.* **2003**, *15*, 353.
(2) Li, H.; Bian, Z.; Zhu, J.; Huo, Y.; Li, H.; Lu, Y. *J. Am. Chem. Soc.* **2007**, *129*, 4538.
(3) Linsebigler, A. L.; Lu, G. Q.; Yates, J. T. *Chem. Rev.* **1995**, *95*, 735.
(4) Brinker, C. J.; Scherer, G. W. *Sol-gel science: The physics and chemistry of sol-gel processing*; Academic Press, Boston, 1990.
(5) (a) Terashima, M.; Inoue, N.; Kashiwabara, S.; Fujumoto, R. *Appl. Surf. Sci.* **2001**, *167*, 535. (b) Ishikawa, Y.; Matsumoto, Y. *Electrochim. Acta* **2001**, *46*, 2819.
(6) Yang, P. D.; Zhao, D. Y.; Margolese, D. I.; Chmelka, B. F.; Stucky, G. D. *Nature* **1998**, *396*, 152.
(7) (a) Kim, D. H.; Sun, Z.; Russell, T. P.; Knoll, W.; Gutmann, J. S. *Adv Funct. Mater.* **2005**, *15*, 1160. (b) Cheng, Y. J.; Gutmann, J. S. *J. Am. Chem. Soc.* **2006**, *128*, 4658.
(8) Kang, Y.; Erickson, K. J.; Taton, T. A. J. *Am Chem. Soc.* **2005**, *127*, 13800.
(9) Cui, H.; Chen, Z.; Zhong, S.; Wooley, K. L.; Pochan, D. J. *Science* **2007**, *317*, 647.
(10) Brandrup, J., Immergut, E. H., Grulke, E. A., Abe, A., Bloch, D. R., Eds. *Polymer Handbook*, 4th ed.; John Wiley & Sons: New York, 1999.

10.1021/cm7026042 CCC: $40.75

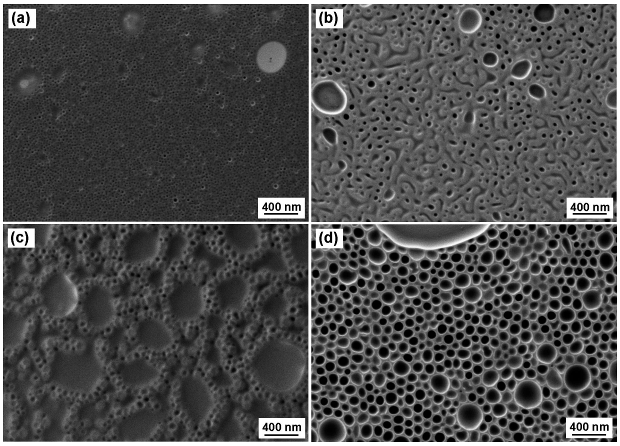

Figure 1. FESEM images of PS-b-P2VP/titania hybrid films with different amounts of sol–gel precursor relative to the BCP content: (a) 11.6%; (b) 23.2%; (c) 46.4%; and (d) 58.0%.

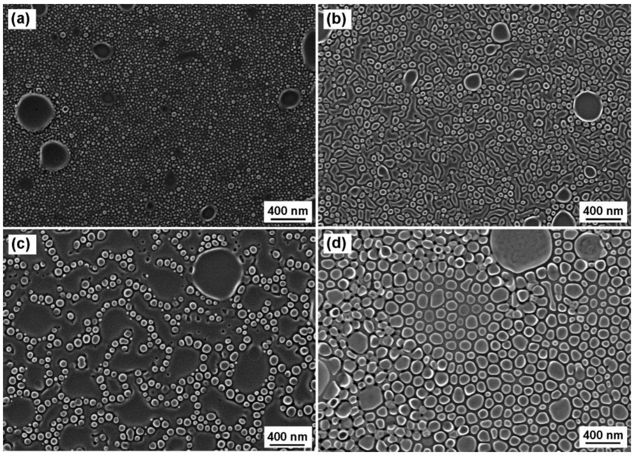

Figure 2. FESEM images of titania nanopatterns prepared from PS-b-P2VP films with (a) 11.6%; (b) 23.2%; (c) 46.4%; and (d) 58.0% sol–gel precursor, after being treated with UV light.

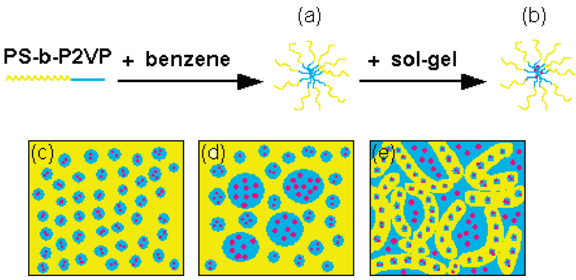

Figure 3. Schematic illustration to fabricate strings of PS-b-P2VP/sol–gel hybrid nanoparticles based on cooperative BCP self-assembly and sol–gel process. (a) Formation of micellar solution of PS-b-P2VP copolymer in benzene. (b) Incorporation of titania precursors into the P2VP domains. (c) Formation of circular nanohole morphology at low precursor amount. (d) Some nanoholes become bigger and irregular when the amount of precursor is increased. (e) 2D arrays of strings of nanoholes are formed when the amount of precursor is further increased.

Figure 2 which were obtained from the initial hybrid organic/inorganic films after removing the organic matrix by UV irradiation. It is clearly observed that highly dense arrays of titania nanodots with a diameter and height of ~40.3 and 8.7 nm, respectively, are obtained from the original hybrid film with 11.6% precursor (Figure 2a). In Figure 2b,c, strings of titania nanoparticles are observed at moderate precursor content after the same UV treatment. It is noteworthy that nanoholes are found at the center of some nanodots like donuts. At higher precursor content, titania nanodots with larger diameter are obtained (Figure 2d).

The evolution of a series of PS-b-P2VP/titania hybrid morphologies in Figure 1 can be explained by understanding the role of sol–gel precursor solution in the mixed solution. Both HCl and titania precursor contribute such unique morphological evolution. It has been reported that acetic acid or hydrofluoric acid selectively swells minor domains in PS-b-PVP leading to depression or opening of pores in PVP nanodomains.[11,12] Therefore, it is reasonable to conclude the HCl in the current system is responsible for the opening of pores, that is, depression at the center of each P2VP nanodomain, in the micelle. At the same time, TTIP is incorporated into the P2VP nanodomains through coordination bonds, hydrolyzed, and condensed into Ti−O− nanostructures. When the content of the TTIP precursor is low, it is uniformly distributed in each P2VP domain, resulting in nanoholes of uniform size as shown in Figure 1a. The uniform nanoholes become bigger and deformed with the incorporation of more titania precursors (Figure 1b). When the amount of precursor is increased further, some adjacent P2VP domains merge together to form bigger holes due to the contact between neighboring titania precursors and push the other P2VP domains align into 2D arrays of strings of nanoholes (Figure 1c). Finally, macrophase separation between the copolymer and the sol–gel solution occurs at 58.0% precursor content. Outside the boundary of the macrophase separation, that is, precursor content higher than ~60%, a more regular network is formed (Figure 1d). On the basis of the experimental observation and mechanism of the structural evolution discussed above, the overall scheme adopted in this study is depicted in Figure 3.

Once the hybrid PS-b-P2VP/titania films in Figure 1 are subjected to UV light, the organic matrix is etched out, leaving behind pure titania domains (Figure 2). It is well-known that UV exposure is an effective mean to selectively eliminate the polymer matrix.[13] The resulting titania structure obtained in this manner proved to be amorphous in nature, which can be converted into anatase phase upon calcination at higher temperature.[14] During the UV exposure, the films attain stable morphology, where the titania nanodomains aggregate to form a spherical nanodot shape. Here, some donut-like structures are observed with the depression at the center of the nanodots, as evidenced in Figure 2b,c. We also provide atomic force microscopy images of the intermediate and the final TiO_2 structures by which a distinct comparison between the hybrid and pure inorganic structures can be made (see Supporting Information). The overall morphology of the resulting titania nanostructures, for example, the portion of nanodonuts, the diameter, depth, and curvature of the

---

(11) Li, X.; Tian, S.; Ping, Y.; Kim, D. H.; Knoll, W. *Langmuir* **2005**, *21*, 9393.

(12) Qiao, Y.; Wang, D.; Buriak, J. M. *Nano Lett.* **2007**, *7*, 464.

(13) Phely-Bobin, T. S.; Muisener, R. J.; Koberstein, J. T.; Papadimitrakopoulos, F. *Adv. Mater.* **2000**, *12*, 1257.

(14) Sun, Z; Kim, D. H.; Wolkenhauer, M.; Bumbu, G.-G.; Knoll, W.; Gutmann, J. S. *ChemPhysChem* **2006**, *7*, 370.

nanohole and nanodot, and so forth, should be a complicated function of the processing parameters such as the relative ratio of the ingredients in mixed solution and the degree of UV exposure.

In summary, an unprecedented path to synthesize 2D arrays of strings of TiO_2 nanoparticles was developed from cooperative self-assembly of PS-b-P2VP copolymer and TTIP-based sol–gel precursors. At first, hybrid BCP/titania thin films with nanohole and nanonetwork morphologies, depending on the relative composition of the mixed solution, were obtained by one-step spin coating of the mixed solution on silicon wafers. During the removal step of organic matrix by exposure to UV light, TiO_2 moieties merged to form spherical nanoparticles where nanoholes are present at the center of individual nanoparticles. This work reports a rare scheme to induce 2D arrays of strings of TiO_2 nanoparticles based on cooperative BCP self-assembly that can be extended to obtain a wide range of inorganic nanostructures with tailored composition, size, and shape.

Acknowledgment. This work was supported by Max Planck Society. J.P. is grateful to the finacial support of Alexander von Humboldt Foundation. D.H.K. acknowledges the support of Seoul Research and Business Development Program (10816). The authors thank Min-Ah Cha and Mihee Kim for their cooperation regarding the sampling of FESEM and TEM experiments.

Supporting Information Available: Height contrast AFM images (PDF). This material is available via the Internet at http://pubs.acs.org.

CM7026042